Optics and Laser Technology 103 (2018) 193–198

Contents lists available at ScienceDirect

Optics and Laser Technology

journal homepage: www.elsevier.com/locate/optlastec

Full length article

Laser-aided Directed Metal Deposition of Ni-based superalloy powder

Fabrizia Caiazzo

Department of Industrial Engineering, University of Salerno, Via Giovanni Paolo II 132, Fisciano, Italy

ARTICLE INFO

Article history:
Received 1 August 2017
Received in revised form 11 December 2017
Accepted 10 January 2018

Keywords:
Laser Directed Metal Deposition
Superalloy
Repair
Diffusion bonding

ABSTRACT

The subject of repairing Ni-based parts with state-of-the-art technologies is increasingly addressed both for research and industrial purposes, aiming to cost saving mainly in aerospace and automotive. In this frame, laser-aided Directed Metal Deposition (DMD) with injection of powder is investigated in this paper since minimal distortion of the work-piece, reduced heat-affected zones and better surface quality are benefited in comparison with conventional techniques. Actual application to overhaul Ni-based components is aimed, therefore homologous powder is fed by means of a 3-way feeding nozzle over the substrate; a disc laser is used as heat source. The chemical composition of both the substrate and the powder is preliminarily investigated via areal and punctual EDS inspections.

A 2-factor, 2-level experimental plan is drawn to discuss the main effects of the processing variables laser power and processing speed. Namely, the resulting trends are given and compared with similar findings in the literature. Interestingly, dilution as a measure of metal affection is found to be lower than 25%, hence the operating window is deemed to be suitable for both repairing and fabrication of parts. Eventually, repairing by means of side overlapping and multi-level deposition traces on artificial square-shaped grooves is performed: indeed, similar slots are made before DMD to preliminarily remove any local imperfection upon improper casting of the part in the actual industrial process. Although a number of micropores are found, the process is deemed to comply with usual referred standards; in particular, a proper processing window has been found to prevent the occurrence of hot cracking which usually affects the compliance to stress.

1. Introduction

Proper actions are required to the purpose of cost saving, mainly in aerospace and automotive, to keep parts and devices in working order. Indeed, specific damages must be addressed when demanding conditions of temperature, wear and mechanical stresses have been experienced [1]. Also, overhaul of new parts could be required to fix minor local manufacturing imperfection resulting from improper casting.

Since part replacement would result in increased costs for any component of complex geometry, a number of innovative technologies are offered in the literature. Among them, laser-aided Directed Metal Deposition (DMD) in the frame of additive manufacturing is receiving increasing interest and has been developed with different names and similar principles by a number of laboratories and manufacturers, as reported in the literature [2–5]: a laser beam is used as focused heat source to scan the surface, thus creating a melting pool over an existing substrate. Metal impinging the pool is fed concurrently (i.e., in single-stage processing) resulting in metallurgical bonding to the substrate thanks to fusion and diffusion; side overlapping is accomplished to process wider surfaces [6]; multi-layer deposition is required for 3D fabrication. Minimal distortion of the work-piece, reduced heat-affected zones and better surface quality are benefited in comparison with conventional coating and repairing techniques such as arc welding or plasma spraying [7,8]. Even further advantages are achieved in terms of processing speed thanks to new generation high-brightness lasers, with increased beam quality [9]. Enhanced productivity is benefited and grounds are given for automation and reduction of the overall processing time; these features are required in adaptive and flexible manufacturing environments and factories of the future [10].

At present, two possibilities of feedstock are offered: wire and powder, the former being preferred in general for its lower cost and lower probability of oxide content [11], the latter for being flexible in materials and allowing higher precision for local repairing [1] with better surface quality and bonding strength [6,12]. Nevertheless, since a number of processing parameters are involved, a statistical analysis of the responses is usually suggested [13,14]. With this respect, efforts have been made to predict the

E-mail address: f.caiazzo@unisa.it

https://doi.org/10.1016/j.optlastec.2018.01.042
0030-3992/

cross-section of the metal deposition via mathematical models [15,16], based on some level of prior experimental work. Nevertheless, depending on the applications, multi-trace and multi-layer depositions are required to address wide damages, hence a number of further geometrical models and profiles have been discussed to predict the resulting features of overlapping traces [17]. To the specific purpose of repairing of complex parts, a feedback close-loop control has been suggested to maintain uniform thickness of deposition, so to save time for post DMD processing [2].

A wide range of Ni-based components are used in aerospace to benefit from combined mechanical strength, creep rupture properties and resistance to oxidation against demanding stress and temperature [18,19]. Therefore, DMD of superalloys for repairing and overhauling is worth investigating. At first, the subject has been discussed in the literature in the field of laser welding, thus offering a valuable insight to be shifted to additive manufacturing, hence to laser-aided DMD. It has been shown that Laves phases or intermetallics may result from cooling and may ease both the initiation and propagation of microcracks [20]; nevertheless, when properly setting the processing parameters to benefit from lower thermal input (i.e., the ratio of power to speed), the requirements for homologation of welding for aerospace have been matched [21,22] and free of cracking weldability has been proven [23].

Given this background suggesting possible successful results, repair and manufacturing of a wide range of Ni-based superalloys, including CMSX-4, Inconel, NiCrAlY, Rene N4 and Waspaloy, has been investigated by means of laser-aided DMD with metal powder [19]; Ni-coating has been considered even for aluminum powder to improve the process in terms of absorptance, residual porosity and resulting strength [24]. At first, it has been shown that proper care must be taken with respect to virgin Ni-based powder [25]: namely, small particle size and narrow particle size distribution lead to uniform microstructure and high tensile strength; furthermore, residual porosity and crack initiation are affected by laser power. Among other concerns, possible contamination of the parent metal must be restrained, in agreement with general practice on DMD: to this purpose, dilution is usually considered [6,14], to index the result of mixing with the substrate.

In general, a crucial challenge is offered by single crystal superalloys, as deposition lead to formation of stray grains yielding to cracking [26]. Moreover, a further challenge is offered by randomly oriented or curved surfaces which may appear in actual applications of repairing and rapid manufacturing over Ni-based parts, irrespective of their crystalline structure [19].

A face-centred cubic superalloy is considered in this study; strength is enhanced thanks to fine distribution of γ' precipitates $Ni_3(Al,Ti)$ [18]. During solidification and depending on the processing parameters, coarser precipitates result; moreover, Mo and Ti carbides may form along the grain boundaries. As for any Ni-based superalloy, the resulting microstructure of the deposited metal is expected to depend on the direction of processing and the parameters [19]; as a consequence, it may differ from the equilibrium structure due to high cooling rates [2]. A full operational original microstructure must be restored by means of 1190 °C solution heat treating, in vacuum, for one hour [27].

Laser-aided DMD with injection of homologous powder has been investigated in this paper over flat surfaces. The effect of the main processing parameters, power and speed, on the geometry of single-trace depositions has been discussed. A condition of processing, preventing cracking, has been selected to be implemented in multi-trace, multi-layer deposition strategy inside a square-shaped groove, aiming to give grounds for real application of the process in an industrial environment.

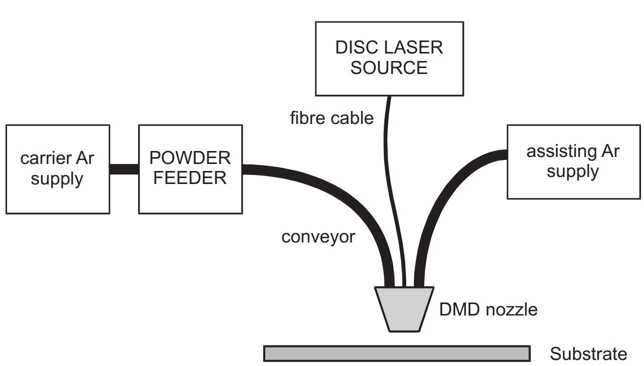

Fig. 1. Laser deposition line, base components.

2. Experimental procedure

2.1. Laser deposition line

To perform DMD for both single- and multi-trace processing, a laser deposition line has been arranged (Fig. 1). A fibre-delivered, Yb:YAG disc laser source, operating in continuous wave emission (Table 1), has been used. The movement of the laser head has been accomplished by means of a 6-axis industrial robot with dedicated controller. An in-built feeding nozzle has been moved with the laser head. A 3-way feeding nozzle, receiving the base metal from a powder feeder with oscillating conveyor, has been used to supply the powder to the deposition line. Thanks to this device, wider and thicker traces are produced with respect to single co- or off-axial feeding, to the purpose of shifting the optimization to real application where throughput instead of precision is crucial; nonetheless, dressing is planned upon DMD to match the nominal dimensions.

Namely, three stream cones of metal powder enclosing the laser beam are provided (Fig. 2); each stream is injected by its separate argon conveying flow. Argon as well, flowing coaxially to the laser beam, has been considered to shield the melting pool from the environment, in agreement with similar applications in the literature [28,29]. A 12 mm stand-off has been allowed between the tip of the feeding nozzle and the reference plane, so that the minimum size of the streams is delivered to the surface of the component. A tilting angle of 4° has been given to the laser head, in agreement with common practice to process metals to prevent back-reflections from entering the optics train.

Since repairing is aimed, homologous powder has been used; gas-atomized Ni-based powder, 50 μm mean particle size, has been used over a substrate of same nominal chemical composition; as a steady feeding rate must be provided consistently, the powder has been preliminarily dried so to flow properly through the conveyor. The chemical composition of both the substrate and the powder has been investigated via Energy Dispersive Spectrometry (EDS) and is given in the relevant section; to this purpose, 15 kV accelerating voltage, 1nA probe current and 3 min probing live time have been set.

An indenting load of 0.200 kg has been used for a dwell period of 10 s to perform Vickers micro-hardness testing.

Table 1
Main technical features of the laser system.

Parameter	Value
Maximum output power [kW]	4.0
Operating nominal wavelength [nm]	1030
Beam parameter product [mm × mrad]	8.0
Core diameter of the delivering fibre [μm]	300
Spot size of the laser beam on the surface [mm]	3
Spot size of the powder stream [mm]	2.5

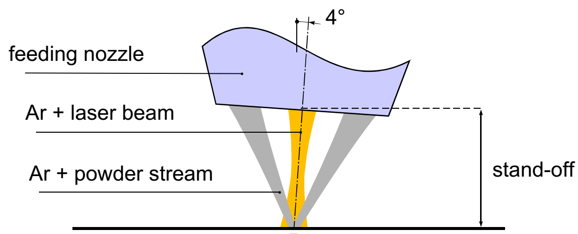

Fig. 2. Scheme of the 3-way feeding nozzle; the items are not to scale.

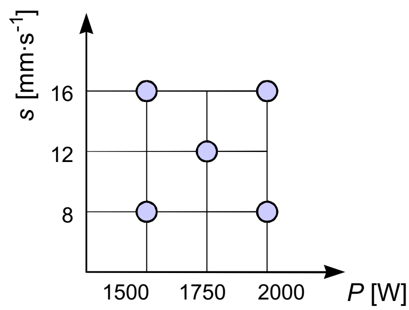

Fig. 3. Processing conditions in preliminary trials.

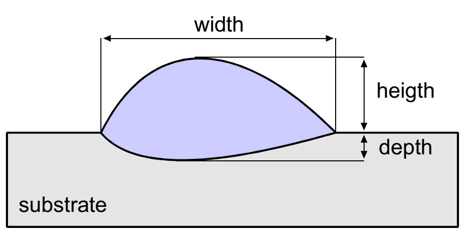

Fig. 4. Scheme of the geometrical responses in the cross-section.

2.2. Governing factors and responses

At first stage, preliminary trials in form of single deposition over 3.3 mm thick Ni-based plates have been conducted to investigate the response of the base metal to laser-aided DMD with injection of homologous powder. The main input variables have been selected based on the referred literature: the effects of laser power P and laser scanning speed s have been discussed. A full-factorial, 2-factor, 2-level experimental plan has been considered, with the addition of the central point (Fig. 3); according to the literature [30] and previous studies [14] on DMD of metal powder, setting a 2-level plan is expected to be valid, as only weak interactions are in place. Therefore, five processing conditions of trial resulted; three replications have been considered for each testing point to evaluate the average responses. A random testing procedure has been arranged.

The general approach to find the operating window is given in the following. In terms of specific delivered power and feeding, the processing levels are deemed to agree with a similar work in the literature [28]. Nevertheless, these have been properly adjusted so to result in valuable outcomes (i.e., preventing detachment, balling, lack of clad, excessive dilution or surface oxidation of the traces). Namely, with respect to speed, this must be taken below a threshold value so to promote homogenization of the interface between trace and substrate [6,12]; power has been adjusted in turn to reduce the thermal affection in the base material. Defocusing of the laser beam has been set to 28 mm to improve catchment, which is crucial when DMD is performed by powder injection [6]; namely, the size of the melting pool has been increased from a focus beam diameter of 0.3 mm to a processing beam diameter of 3 mm over the substrate, so to match the size of the powder stream cones. Lower irradiance has been benefited as well, to the purpose of reduced penetration depth and dilution in turn. The flow rate for both carrier and shielding argon has been taken as a constant, 3 and 10 l min^{-1}, respectively, thus allowing a required given powder feeding rate of 13 g min^{-1}.

The geometry as a function of the processing parameters has been discussed: in agreement with common practice in DMD, trace width in the cross-section, depth and height with respect to the reference plane have been measured (Fig. 4) over three specimens for each sample in order to assess the main effects and a proper processing condition to perform overlapping, multi-layer repairing.

Moreover, dilution must be investigated. Although a chemical definition is usually given involving the weight percentage composition of the main alloying elements in the substrate with respect to the reported metal [6], it has been shown that an alternative geometric definition can be given [31]; namely, the ratio of the fused (i.e., mixing) area of the substrate to the total area in the transverse cross-section can be measured. To a first approximation [32], this can be even given as:

$$\text{dilution} = \frac{\text{depth}}{\text{height} + \text{depth}}$$

The geometrical approximation involving depth and height has been referred in this work.

3. Results and discussion

3.1. Composition

The powder has been preliminarily inspected in terms of size and geometry, since specific requirements of shape must be matched to the purpose of proper manufacturing. Spherical and near-spherical particles have been found (Fig. 5), thus efficient flowability and layer packaging are expected to result in uniform melting.

The chemical composition of both the substrate and the powder has been investigated via areal and punctual EDS inspections. An average overall fitting coefficient of the quantitative analysis (i.e., the residual between the acquired and the synthetic spectra) of 2.4% and 2.5% resulted for the substrate and the powder, respectively; certain elements below 1% wt. have not been detected (see Table 2).

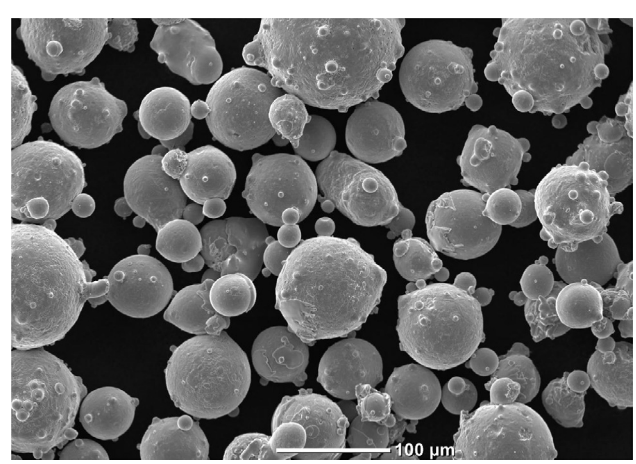

Fig. 5. Electron microscopy of pre-alloyed, argon gas-atomized, virgin Ni-based powder.

Table 2
Average chemical composition (wt.%) of substrate and virgin powder resulting from EDS inspections.

	Ni	Cr	Co	Mo	Al	Ti
Substrate	59.4	14.8	10.6	7.7	4.5	3.0
Powder	58.4	15.5	10.3	8.3	4.0	3.5

Table 3
Details of the traces for each processing condition.

Power [W]	Speed [mm s^{-1}]	Trace aspects
1500	16	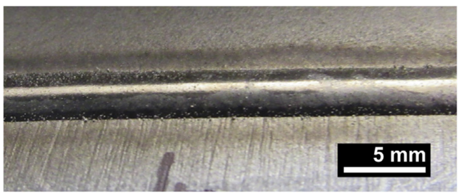
2000	16	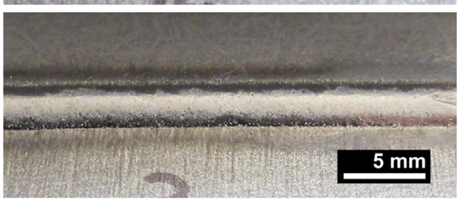
1750	12	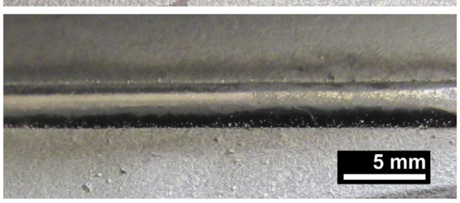
1500	8	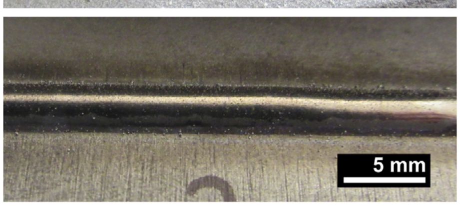
2000	8	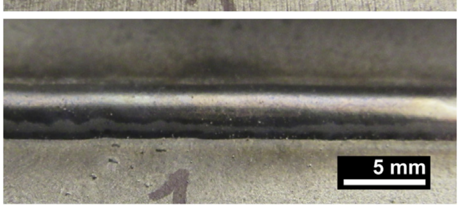

3.2. Single-trace deposition

Based on visual inspections (Table 3), all of the conditions of the experimental plan resulted in successful processing, therefore inert shielding is deemed to be effective. The deposited metal has been found to be sound, at macroscopical scale at least. Nevertheless, a number of indications (i.e., surface cracks) have been found via Fluorescent Penetrant Inspection (FPI). These are mostly common when the conditions with higher thermal input are investigated. Based on this, the condition with 1.5 kW power, 16 mm s^{-1} speed, resulting in the lowest thermal input (approx. 95 J mm^{-1}) within the investigating domain should be selected.

Additional reasons can be given to support the need for this. Indeed, it has been said in the literature [33] that large grain size in conventionally casted nickel-based superalloys may result in quasi-brittle fracture; therefore, a finer structure must be aimed by means of shorter time for cooling, hence lower thermal input. Furthermore, with respect to laser net-shape manufacturing of Inconel 718 parts, it has been shown [4] that since a lower heat input results in shorter time for cooling, less Laves phases are produced, with increased material properties.

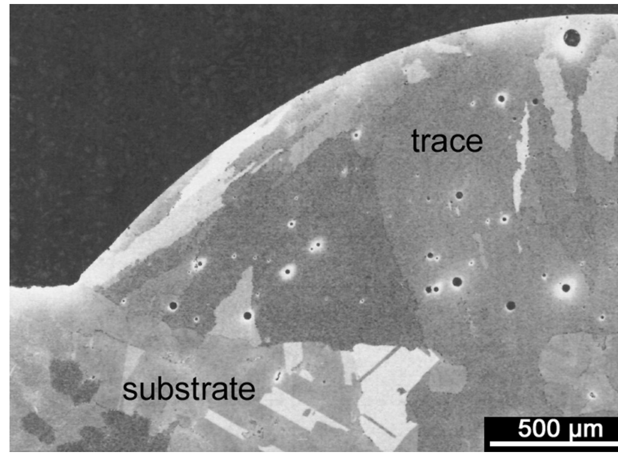

Fig. 6. Micropores in the fusion zone (1.5 kW laser power, 16 mm s^{-1} speed).

As regarding the soundness at microscopical scale, a number of micropores, 60 µm at most in size, have been found in the cross-section (Fig. 6). One may assume this would not result in rejection at quality checks. Indeed, since no specific regulations are currently available for DMD, usual international standards for quality in laser welding [34] have been borrowed: the standard is matched in terms of allowed pore size and accumulated length. Interestingly, the total amount of pores did not show any correlation with the processing parameters, therefore a random source must be ascribed to; with this respect, it has been suggested that pores may be induced by trapped processing gases [25].

Irrespective of their possible imperfections in terms of cracks and porosity, all of the processing conditions of the experimental plan are valuable to draw a general overview of the process in terms of dependence on the governing factors. Trace width, depth, height and dilution have been measured (Table 4) and discussed via main effect plots (Fig. 7) as a function of the processing parameters.

As expected, width is found to increase for increasing power, decrease for increasing speed otherwise, as a reduced thermal input is provided. The same reasons apply for depth. As regarding the height, an increase of power yields a decrease in height as a larger pool is induced; therefore powder is laid over a wider trace. On the other hand, an increase in speed yields a decrease in height since the feeding nozzle is moved with the laser head, hence less powder is laid per unit length. Dilution is found to be lower than 25%, hence the operating window is deemed to be suitable for both repairing and fabrication of parts; its trend results from concurrent effects of the governing factors on depth and height. All of the trends are in agreement with similar findings on DMD of metals [14,35]. For each response, no interactions among the governing factors are inferred based on the interaction plots, therefore the choice of a 2-level plan is deemed to be consistent and effective.

3.3. Multi-trace repairing

Based on the outcome of the experimental plan, the condition with 1.5 kW power, 16 mm s^{-1} speed has been selected to perform multi-trace repairing over 15 mm long, 6 mm wide and 2 mm deep square-shaped grooves produced by means of face milling. In the actual industrial process, similar slots are made before DMD to

Table 4
Average geometrical responses for each processing condition.

Power [W]	Speed [mm s^{-1}]	Width [mm]	Depth [mm]	Height [mm]	Dilution [%]
1500	16	3.43	0.20	0.80	20%
2000	16	3.59	0.22	0.71	24%
1750	12	3.64	0.28	0.90	24%
1500	8	3.95	0.31	1.54	17%
2000	8	4.15	0.34	1.23	22%

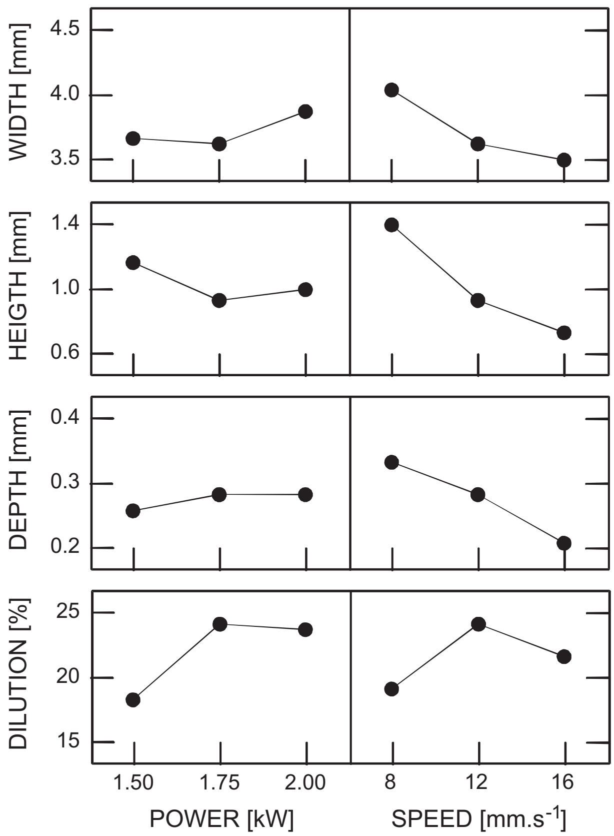

Fig. 7. Main effect plots for mean responses as a function of the governing factors.

preliminarily remove any local imperfection upon improper casting of the part, indeed. Side overlapping and multi-level deposition traces have been required (Fig. 8). Namely, three traces have been performed over each layer of deposition and an offset of the direction of deposition (i.e., the hatch spacing) has been set to provide partial overlapping and uniform addition of metal in the cross-section. Given that a 3.4 mm wide trace is expected (Table 4), the offset between consecutive depositions has been set to 2 mm, thus resulting in a 40% overlapping ratio; hence three traces have been required to cover each layer of deposition. Furthermore, four layers have been processed so to fill the slot: the order of deposition is the same in any layer; the stand-off has been progressively increased of 0.8 mm (i.e., the expected height in single deposition), hence the nominal processing diameter has been taken over the top surface.

Upon single- and multi-trace processing, solution heat treating at 1190 °C, in vacuum, for one hour has been performed; then, non-destructive tests in form of FPI have been conducted. With respect to repairing, eventual post-processing of the machining allowance (i.e., part of the last deposition exceeding the groove) has been required.

Uniform fusion resulted (Fig. 9); the total percentage of pores has been found to be consistent with respect to the single-trace counterpart. As a consequence, the referred standard [34] is still matched. One may infer the process can be successfully shifted from single- to multi-trace depositions within a defined bound. Interestingly, a decrease of Vickers micro-hardness in a measure of 12% on average resulted in the fusion zone (375 $HV_{0.2}$) with respect to the base metal (425 $HV_{0.2}$): indeed, although homogeneous material is delivered to the substrate, new microstructures are formed as a consequence of different cooling rates, similarly to welding [23].

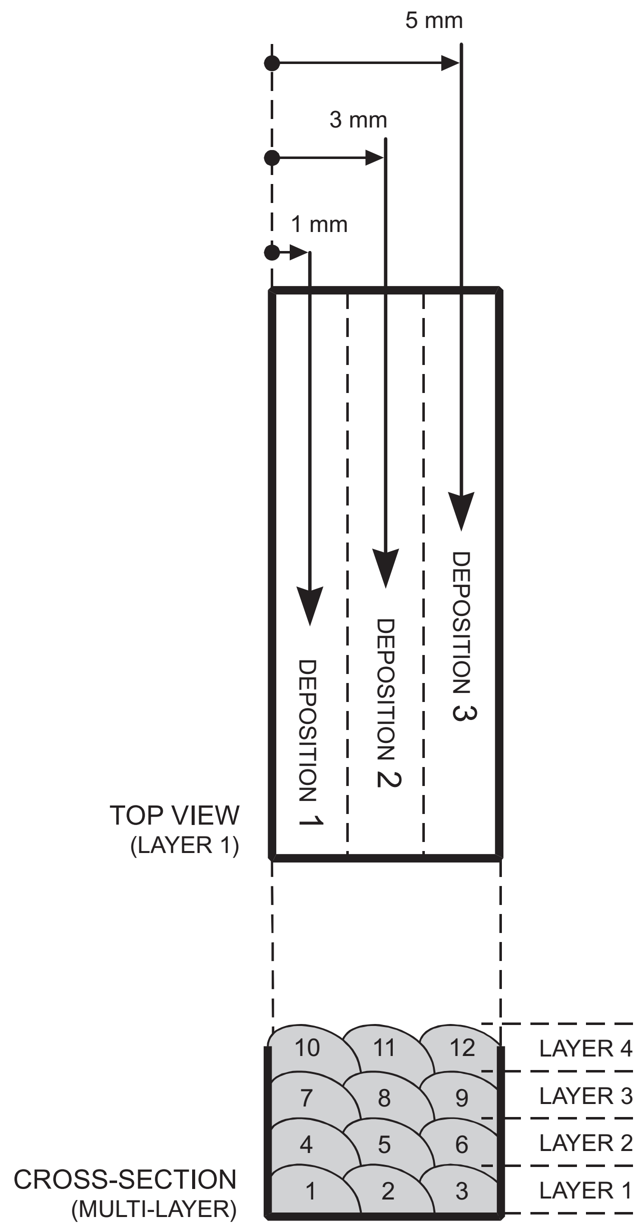

Fig. 8. Scheme of the deposition strategy; consecutive numbers are indicative of the order of trace deposition.

Fig. 9. Longitudinal cross-section of the groove upon repairing and milling of the allowance.

4. Conclusions

In this paper, the effectiveness of DMD of Ni-based powder over homologous surfaces has been proven. The trends of the main responses as a function of the main governing factors power and speed have been discussed; it has been shown that dilution can be restrained below 25%, hence resulting in low affection of the base metal. In this frame, upon preliminary investigation of single-trace depositions, a proper processing condition has been found; it is worth noting that although wider and higher traces may result otherwise, higher thermal input would be required, with consequent possible cracks and increased amount of detrimental Laves phases.

In agreement with similar findings in the literature about Ni-based superalloy, a condition with low thermal input has been preferred indeed, then shifted to multi-trace repairing within a defined bound. A square-shaped groove slot has been repaired. Although a number of micropores have been found, the process is deemed to comply with usual referred standards.

Acknowledgements

The author gratefully acknowledge the financial support from the Italian Ministry for University and Research (MIUR) for funding this research activity through PON03PE_00111_1 MATEMI; eng. Vittorio Alfieri for his valuable contribution to the research.

References

[1] A. Riveiro, A. Mejías, F. Lusquiños, J. del Val, R. Comesaña, J. Pardo, J. Pou, Laser cladding of aluminium on AlSi 304 stainless steel with high-power diode lasers, Surf. Coat. Technol. 253 (2014) 214–220.
[2] G.P. Dinda, A.K. Dasgupta, J. Mazumder, Laser aided direct metal deposition of Inconel 625 superalloy – Microstructural evolution and thermal stability, Mater. Sci. Eng., A 509 (1–2) (2009) 98–104.
[3] J. Chen, L. Xue, Process-induced microstructural characteristics of laser consolidated IN-738 superalloy, Mater. Sci. Eng., A 527 (2010) 7318–7328.
[4] H. Qi, M. Azer, A. Ritter, Studies of standard heat treatment effects on microstructure and mechanical properties of laser net shape manufactured Inconel 718, Metall. Mater. Trans. A 40 (2009) 2410–2422.
[5] H. El Cheikh, B. Courant, S. Branchu, J. Hascoet, R. Guillen, Analysis and prediction of single laser tracks geometrical characteristics in coaxial laser cladding process, Opt. Lasers Eng. 50 (2012) 413–422.
[6] E. Toyserkani, A. Khajepour, S. Corbin, Laser Cladding, CRC Press, Boca Raton, 2005.
[7] B. Cárcel, A. Serrano, J. Zambrano, V. Amigó, A.C. Cárcel, Laser cladding of TiAl intermetallic alloy on Ti6Al4V, process optimization and properties, Phys. Proc. 56 (2014) 284–293.
[8] I. Tabernero, A. Lamikiz, S. Martinez, E. Ukar, J. Figueras, Evaluation of the mechaanical properties of Inconel 718 components built by laser cladding, Int. J. Mach. Tools Manuf. 51 (2011) 465–470.
[9] J. del Val, R. Comesaña, F. Lusquiños, M. Boutinguiza, A. Riveiro, F. Quintero, J. Pou, Laser cladding of Co-based superalloy coatings: comparative study between Nd:YAG laser and fibre laser, Surf. Coat. Technol. 204 (2010) 1957–1961.
[10] A. Radziwon, A. Bilberg, M. Bogers, E. Madsen, The smart factory: exploring adaptive and flexible manufacturing solutions, Proc. Eng. 69 (2014) 1184–1190.
[11] N.I.S. Hussein, J. Segal, D.G. McCartney, I.R. Pashby, Microstructure formation in Waspaloy multilayer builds following direct metal deposition with laser and wire, Mater. Sci. Eng., A 497 (2008) 260–269.
[12] W. Steen, J. Mazumder, Laser material processing, Springer, London, 2010.
[13] A. Angelastro, S.L. Campanelli, G. Casalino, Statistical analysis and optimization of direct metal laser deposition of 227-F Colmonoy nickel alloy, Opt. Laser Technol. 94 (2017) 138–145.
[14] F. Caiazzo, V. Alfieri, P. Argenio, V. Sergi, Additive manufacturing by means of laser-aided directed metal deposition of 2024 aluminium powder: investigation and optimization, Adv. Mech. Eng. 9 (6) (2017) 1–12.
[15] R. Reed, The superalloys, Cambridge University Press, New York, Fundamentals and Applications, 2006.
[16] H. El Cheikh, B. Courant, J. Hascoet, R. Guillen, Prediction and analytical description of the single laser track geometry in direct laser fabrication from process parameters and energy balance reasoning, J. Mater. Process. Technol. 212 (2012) 1832–1839.
[17] O. Nenadl, W. Kuipers, N. Koelewijn, V. Ocelik, J. De Hosson, A versatile model for the prediction of complex geometry in 3D direct laser deposition, Surf. Coat. Technol. 307A (2016) 292–300.
[18] V. Ocelik, O. Nenadl, A. Palavra, J. De Hosson, On the geometry of coating layers formed by overlap, Surf. Coat. Technol. 242 (2014) 54–61.
[19] R. Vilar, A. Almeida, Repair and manufacturing of single crystal Ni-based superalloys components by laser powder deposition – A review, J. Laser Appl. 27 (2015) 1–7.
[20] X.B. Liu, G. Yu, J. Guo, Y.J. Gu, M. Pang, C.Y. Zheng, H.H. Wang, Research on laser welding of cast Ni-based superalloy K418 turbo disk and alloy steel 42CrMo shaft, J. Alloy. Compd. 453 (2008) 371–378.
[21] F. Zapirain, F. Zubiri, F. Garciandia, I. Tolosa, S. Chueca, A. Goiria, Development of laser welding of Ni based superalloys for aeronautic engine applications (experimental process and obtained properties), Phys. Proc. 12 (2011) 105–112.
[22] F. Caiazzo, V. Alfieri, V. Sergi, A. Schipani, S. Cinque, Dissimilar autogenous disk-laser welding of Haynes 188 and Inconel 718 superalloys for aerospace applications, Int. J. Adv. Manuf. Technol. 38 (5/8) (2013) 1809–1820.
[23] F. Caiazzo, V. Alfieri, V. Sergi, A. Tartaglia, M. Di Foggia, A. Niola, Technical feasibility of laser dissimilar welding of superalloys on casted nozzle guide vanes, Proc. CIRP 41 (2016) 963–968.
[24] A. Singh, A. Ramakrishnan, D. Baker, A. Biswas, G.P. Dinda, Laser metal deposition of nickel coated Al 7050 alloy, J. Alloy. Compd. 719 (2017) 151–158.
[25] Y. Kakinuma, M. Mori, Y. Oda, T. Mori, M. Kashihara, A. Hansel, M. Fujishima, Influence of metal powder characteristics on product quality with directed energy deposition of Inconel 625, CIRP Ann. – Manuf. Technol. 65 (1) (2016) 209–212.
[26] M.B. Henderson, D. Arrell, R. Larsson, M. Heobel, G. Marchant, Nickel based superalloy welding practices for industrial gas turbine applications, Sci. Technol. Weld. Joining 9 (1) (2004) 13–21.
[27] I. Hernandez, A. Subinas, I. Madariaga, K. Ostolaza, Improving C1023 manufacturability using two-step heat treatment, Heat Treat. Prog. 3 (2007) 25–31.
[28] C.P. Paul, P. Ganesh, S.K. Mishra, P. Bhargava, J. Negi, A.K. Nath, Investigating laser rapid manufacturing for Inconel-625 components, Opt. Laser Technol. 39 (2007) 800–805.
[29] Q. Zhang, J. Yao, J. Mazumder, Laser direct metal deposition technology and microstructure and composition segregation of Inconel 718 superalloy, J. Iron. Steel Res. Int. 18 (4) (2011) 73–78.
[30] B. Graf, S. Ammer, A. Gumenyuk, M. Rethmeier, Design of experiments for laser metal deposition in maintenance, repair and overhaul applications, Proc. CIRP 11 (2013) 243–248.
[31] G. Abbas, D. West, Laser surface cladding of stellite and stellite-SiC composite deposits for enhanced hardness and wear, Wear 143 (1991) 353–363.
[32] W. Ya, B. Pathiraj, S. Liu, 2D modelling of clad geometry and resulting thermal cycles during laser cladding, J. Mater. Process. Technol. 230 (2016) 217–232.
[33] K.M. Kraemer, F. Mueller, M. Oechsner, Application-oriented description of time-/temperature dependent crack growth in a conventionally cast nickel-based superalloy, Int. J. Fatigue 96 (2017) 78–88.
[34] American Welding Society, D17.1 – Specification for Fusion Welding for Aerospace Applications. AWS, Miami, 2001.
[35] A. Riveiro, A. Mejías, F. Lusquiños, J. del Val, R. Comesaña, J. Pardo, J. Poub, Optimization of laser cladding for Al coating production, Phys. Proc. 41 (2013) 327–334.